



**HAL**  
open science

## A ternary complex of Hydroxycinnamoyl-CoA Hydratase-Lyase (HCHL) with acetyl-Coenzyme A and vanillin gives insights into substrate specificity and mechanism.

Joseph P. Bennett, Lucille Bertin, Benjamin Moulton, Ian J.S. Fairlamb, A. Marek Brzozowski, Nicholas J. Walton, Gideon Grogan

### ► To cite this version:

Joseph P. Bennett, Lucille Bertin, Benjamin Moulton, Ian J.S. Fairlamb, A. Marek Brzozowski, et al.. A ternary complex of Hydroxycinnamoyl-CoA Hydratase-Lyase (HCHL) with acetyl-Coenzyme A and vanillin gives insights into substrate specificity and mechanism.. *Biochemical Journal*, 2008, 414 (2), pp.281-289. 10.1042/BJ20080714 . hal-00479007

**HAL Id: hal-00479007**

**<https://hal.science/hal-00479007>**

Submitted on 30 Apr 2010

**HAL** is a multi-disciplinary open access archive for the deposit and dissemination of scientific research documents, whether they are published or not. The documents may come from teaching and research institutions in France or abroad, or from public or private research centers.

L'archive ouverte pluridisciplinaire **HAL**, est destinée au dépôt et à la diffusion de documents scientifiques de niveau recherche, publiés ou non, émanant des établissements d'enseignement et de recherche français ou étrangers, des laboratoires publics ou privés.

A ternary complex of Hydroxycinnamoyl-CoA Hydratase-Lyase (HCHL) with acetyl-Coenzyme A and vanillin gives insights into substrate specificity and mechanism.

Joseph P. Bennett,\* Lucille Bertin,\* Benjamin Moulton,† Ian J.S. Fairlamb,† A. Marek Brzozowski,\* Nicholas J. Walton‡ and Gideon Grogan\*

\*York Structural Biology Laboratory, Department of Chemistry, University of York, Heslington, York, YO10 5YW U.K.

†Department of Chemistry, University of York, Heslington, York, YO10 5DD U.K.

‡Institute of Food Research, Norwich Research Park, Colney, Norwich, NR4 7UA U.K.

Corresponding author: [grogan@ysbl.york.ac.uk](mailto:grogan@ysbl.york.ac.uk); Tel: 44 1904 328256; Fax: 01904 3282666

Short Title: Ligand Complexes of HCHL

Keywords: Vanillin, Crotonase, Hydratase, Lyase, Aldolase

## Synopsis

Hydroxycinnamoyl-CoA Hydratase-Lyase (HCHL) catalyses the biotransformation of feruloyl-CoA to acetyl-CoA and the important flavour-fragrance compound vanillin (4-hydroxy 3-methoxybenzaldehyde) and is exploited in whole-cell systems for the bioconversion of ferulic acid to natural-equivalent vanillin. The reaction catalysed by HCHL has been thought to proceed by a two-step process involving first the hydration of the double bond of feruloyl-CoA, then the cleavage of the resultant beta-hydroxy thioester by *retro*-aldol reaction to yield the products. Kinetic analysis of active site residues identified using the crystal structure of HCHL revealed that whilst Glu-143 was essential for activity, Ser-123 played no major role in catalysis. However, mutation of Tyr-239 to Phe greatly increased the  $K_M$  for the substrate ferulic acid, fulfilling its anticipated role as a factor in substrate binding. Structures of wild-type HCHL and of the Ser123Ala mutant, each of which had been co-crystallised with feruloyl-CoA, reveal a subtle helix movement upon ligand binding, the consequence of which is to bring the phenolic hydroxyl of Tyr-239 into close proximity with Tyr-75 from a neighbouring subunit in order to bind the phenolic hydroxyl of the product vanillin, for which electron density was observed. The active site residues of ligand-bound HCHL display a remarkable three-dimensional overlap with those of a structurally unrelated enzyme, vanillyl alcohol oxidase, that also recognises *para*-hydroxylated aromatic substrates related to vanillin. The data both explain the observed substrate specificity of HCHL for *para*-hydroxylated cinnamate derivatives and illustrate a remarkable convergence of the molecular determinants of ligand recognition between two otherwise unrelated enzymes.

## Introduction

The industrial biosynthesis of the flavour and fragrance component vanillin (4-hydroxy-3-methoxybenzaldehyde) from natural feedstocks is of contemporary interest as it can provide access to the natural-labelled product [1]. The transformation of ferulic acid (4-hydroxy, 3-methoxy-cinnamic acid) to vanillin by bacteria and fungi has proved attractive, as ferulic acid constitutes a high proportion of the material produced as waste from the large scale processing of corn hulls [2]. Several studies have been conducted into the enzymes responsible for the microbial conversion of ferulic acid to vanillin [3-7], and the genes encoding their activities. In 1998, Narbad and Gasson and co-workers described the isolation of a strain of *Pseudomonas fluorescens*, designated AN103, which was able to grow on ferulic acid as sole carbon source [6]. The biotransformation of ferulic acid to vanillin by this strain is summarised in Figure 1. Ferulic acid **1** was first ligated to Coenzyme-A by the action of an ATP-dependent hydroxycinnamic acid-Coenzyme-A ligase (HCLS). The coenzyme A ester of ferulic acid (feruloyl-CoA, Fer-CoA, **2**) was then converted to vanillin **4** by first, a hydration of the double bond at the benzylic position to give 4-hydroxy-3-methoxyphenyl- $\beta$ -hydroxypropionyl-SCoA (HMPHP-CoA **3**), thence cleavage of the  $\beta$ -hydroxy thioester **3** by *retro*-aldol reaction. It was demonstrated [7] that the chemically-synthesised hydrated intermediate **2** was stable under the buffered reaction conditions in the absence of enzyme. Walton and co-workers also demonstrated that both hydration and *retro*-aldol half-reactions could be attributed to the activity of one enzyme, named hydroxycinnamoyl-CoA hydratase-lyase (HCHL). It was also shown that the substrate specificity of HCHL encompassed the Coenzyme-A thioesters of caffeic acid (3,4-dihydroxycinnamic acid) and coumaric acid (4-hydroxycinnamic acid) but not those of syringic acid (3-hydroxyl-2,4-methoxycinnamic acid) or cinnamic acid itself, indicating that a hydroxyl group relatively free of adjacent steric bulk was necessary for substrate recognition [8].

The gene encoding HCHL was cloned and expressed in *E. coli* by Walton and co-workers [7]. Sequencing of the gene revealed HCHL to be a member of the crotonase superfamily of enzymes [9]. The parent enzyme of the crotonase, or low-similarity isomerase-hydratase group, is enoyl-CoA hydratase or crotonase, the enzyme that catalyses the stereospecific hydration of enoyl-CoA in the course of fatty acid metabolism [10]. Other members of this family, the substrates of which are usually acyl-CoA thiesters, catalyse different chemical reactions, including carbon-carbon bond cleavage [11], dehalogenation [12] and decarboxylation [13], but are in each case related both by tertiary fold and the stabilisation of a common enolate formed at the CoA-thioester that is bound within a conserved oxyanion hole formed by the peptidic N-Hs of two residues, separated usually by approximately fifty amino acids in the amino acid sequence. This conservation of mechanistic attribute has been demonstrated using a number of structural studies on, for example, crotonase [14] itself, carboxymethylproline synthase CarB [15] and most recently, the cofactor-independent dioxygenase DpgC [16].

In the interests of illuminating the molecular determinants of both substrate specificity and mechanism in HCHL, we determined the structure of the native *apo*-enzyme from the gene expressed in *E. coli* to a resolution of 1.8Å [17]. HCHL was a hexamer, in common with other members of the crotonase superfamily, and the structure superimposed well with the structure of enoyl-CoA hydratase, with a root-mean-square deviation of 1.64Å for 215 matched residues. Using a structure of ECH complexed with (4-*N*, *N*-dimethyl)cinnamoyl-CoA [18] as a guide, feruloyl-CoA was modelled into the active site of HCHL using the conserved oxyanion hole formed, in the case of HCHL, from the backbone amide nitrogens of Met-70 and Gly-120, to orientate the carbonyl of the acyl-CoA thioester and thus position the ligand.

A comparison of the amino acid sequence of ECH and HCHL revealed that, of the two glutamate residues that had been shown to bind the catalytic water molecule for hydration in ECH, only one, Glu-164, was conserved in HCHL; the other, Glu-144, was replaced by a serine residue (Ser-123) (Figure 2). It was known that, whereas both enzymes catalyse the hydration of carbon-carbon double bonds, only HCHL had been reported to be capable of cleaving the resultant  $\beta$ -hydroxythioester to yield acetyl-CoA and an aldehyde as products. The HCHL model suggested that a catalytic water molecule, bound by Glu-143 and the backbone amide N-H of Gly-151, was suitably positioned to attack the double bond of feruloyl-CoA for the hydration reaction. Ser-123 was estimated to be at a distance of 6-7Å from the site of C-C bond cleavage however. It was also interesting to note that in the model the phenolic hydroxyl of feruloyl-CoA would form a hydrogen bond with the phenol of Tyr-239 of the neighbouring subunit, suggesting a possible determinant of substrate specificity.

It was therefore our intention to investigate, both using structural studies of enzyme-substrate complexes and the kinetic analysis of relevant mutants, the roles of Glu-143 and Ser-123 in hydration and C-C bond cleavage and Tyr-239 in substrate recognition in HCHL. In this report we describe kinetic studies on the recombinant enzyme and the Ser123Ala, Glu143Ala, Ser123Ala/Glu143Ala and Tyr239Phe mutants, in addition to the structures of the WT and Ser123Ala mutant of HCHL in complex with acetyl-CoA and vanillin. These studies have confirmed Glu-143 as essential to catalysis and Tyr239 as an important residue in determining substrate specificity, in addition to revealing domain movements on substrate binding that implicate additional residues in catalysis by HCHL.

## Experimental

### Chemicals

All chemicals were obtained from Sigma (Poole, Dorset, U.K) unless otherwise specified. Feruloyl-CoA was synthesized according to the method of Gasson *et al.* [7]. Detailed analysis of feruloyl-CoA using

both  $^1\text{H}$  and  $^{32}\text{P}$  NMR was performed in order to confirm the identity of the substrate prior to enzyme assay. These are presented in Table 1 and Figure 3 respectively.

### *Plasmids, Bacterial Strains and Culture Conditions*

In previous studies [17] the gene encoding HCHL was expressed using plasmid pIF1009 obtained from the Institute of Food Research. As expression levels were somewhat low, and there was no affinity tag on the expressed gene product, the gene was re-amplified using the genomic DNA from *Pseudomonas fluorescens* AN103 as a template. The primers for PCR amplification were: CCA GGG ACC AGC AAT GAG CAC ATA CGA AGG TCG CTG GAA AAC (forward) and GAG GAG AAG GCG CGT TAT CAG CGT TTA TAC GCT TGC AGG CCA G (reverse). The PCR reaction involved an initial denaturing step at  $94^\circ\text{C}$  for 120 s, followed by 35 cycles of melting ( $94^\circ\text{C}$  for 30s), annealing ( $55^\circ\text{C}$  for 30s) and extension ( $72^\circ\text{C}$  for 90s) followed by a final extension at  $72^\circ\text{C}$  for 180s. The PCR product was cleaned by running on a 0.8% agarose gel, excised and cleaned using a GenElute kit from Sigma. The gene was cloned using a ligation-independent cloning protocol [19] that led to plasmid LB001, which constituted the pETYSBLIC-3C plasmid with the HCHL gene insert plus an N-terminal histidine tag of six residues. Sequencing confirmed the integrity of the HCHL gene within the new construct. Point mutants of HCHL were constructed using plasmid LB001 as template, and the PCR primers detailed in Table 2 in conjunction with a Quickchange kit from Qiagen. These experiments gave rise to plasmids LB002 (Ser123Ala mutant); LB003 (Glu143Ala mutant) LB004 (Tyr239Phe mutant);. In order to prepare double mutant S123A/E143, LB002 was used as the template, with the primers for the Glu143Ala mutant above. This resulted in plasmid LB005 (Ser123Ala/Glu143Ala mutant).

Procedures for transformation, cell growth and enzyme purification were identical for wild-type HCHL and the relevant mutants. Plasmids were routinely transformed into competent *E. coli* BL21 (DE3), purchased from Novagen using the procedure provided with the cells. Transformants were plated out onto Luria-Bertani (LB) agar containing  $30\ \mu\text{g}\ \mu\text{L}^{-1}$  kanamycin. For preparative cell growth, a single colony from a transformation plate was picked and inoculated into 5 ml of LB medium with  $30\ \mu\text{g}\ \mu\text{L}^{-1}$  kanamycin and grown overnight with shaking at  $37^\circ\text{C}$ . This starter was used to inoculate 500 mL of LB broth containing  $30\ \mu\text{g}\ \mu\text{L}^{-1}$  kanamycin. The culture was grown at  $37^\circ\text{C}$  with shaking until an absorbance ( $A_{600}$ ) of 0.5 was attained. Expression of the gene encoding HCHL was then induced by the addition of 1 mM isopropylthiogalactopyranoside (IPTG). The 500 mL cultures were then incubated with shaking at  $20^\circ\text{C}$  overnight.

### *Isolation of pure wild-type HCHL and mutants*

Cells from 4 x 500 mL cultures were centrifuged at 4000 r.p.m. for 20 minutes and the cell pellets resuspended in 100 mL of 50 mM Tris/HCl buffer pH 7.1 containing 300 mM sodium chloride and 20  $\mu\text{M}$  phenylmethylsulfonyl fluoride (PMSF), henceforth referred to as 'buffer'. The cell suspension was sonicated and the cell debris removed by centrifugation at 15,000 r.p.m for 20 minutes. The soluble fraction was clarified by filtration through a membrane with a pore size of 0.2  $\mu\text{M}$  and the filtrate loaded onto a 5 mL nickel agarose affinity column that had been charged with 0.1M nickel sulphate then equilibrated with the buffer. After loading the protein solution, the column was washed with five column volumes of the buffer containing 30 mM imidazole. The column was then eluted with a gradient of 30 to 500 mM imidazole in the buffer. Fractions containing HCHL were identified by SDS-PAGE and pooled for further purification. The pooled fractions were then concentrated using centricons with a molecular-weight cut-off of 10 kDa to a volume of approximately 10 mL and subjected to further purification using a Hiload 16/60 Sephadex S200 S-200 size exclusion column of volume 120 mL, using the buffer as eluant. Fractions containing HCHL were identified by SDS-PAGE and the protein concentrated using centricons with a molecular-weight cut-off of 10 kDa to a final concentration of approximately  $10\ \text{mg}\ \text{mL}^{-1}$ .

In order to produce protein for crystallization, the histidine tags were removed. The pET-YSBLIC3C vector encodes a cleavage site rendering the N-terminal histidine tag cleavable by 3C protease. To solution of HCHL at a concentration of 1 mg mL<sup>-1</sup> in the buffer was added 3C protease (Novagen) in a ratio of HCHL:3C protease of 200:1. The mixture was incubated at 4°C for 72h with gentle agitation on a blood mixer. The His-tag cleaved protein was isolated by running on a 5 mL nickel affinity column as described above and recovering the flow-through fractions that contained the protein of interest.

#### *Assay of Wild-Type HCHL and Mutants*

Wild-type HCHL and mutants were assayed for their ability to metabolise feruloyl-CoA using the method of Mitra and co-workers [8]. Briefly, to a 1mL quartz cuvette were added 930 µL (or 880 µL in the case of Tyr239Phe) of 0.1 M Tris/HCl buffer pH 8.5 and 50 µL of a solution of feruloyl-CoA of a suitable stock concentration. To this was added 20 µL of a 0.015 mg mL<sup>-1</sup> solution (WT), 20 µL of a 0.03 mg mL<sup>-1</sup> solution (S123A) or 100 µL of a 0.04 mg mL<sup>-1</sup> solution (Y239F). In order to establish Michaelis-Menten plots for the enzymes, initial rates, monitored at an absorbance of 400 nm and a temperature of 25°C, were measured at substrate concentrations of 1, 2, 4, 8, 10, 12, 16, 20, 24, 32, 40, 60 and 80 µM; All runs were performed in triplicate. An extinction coefficient for feruloyl-CoA of 7.2 × 10<sup>3</sup> mol<sup>-1</sup> dm<sup>3</sup> cm<sup>-1</sup> was used in the calculation of kinetic parameters [8].

#### *Crystallisation*

Crystals of Wild-type HCHL and mutants Ser123Ala, Glu143Ala and Ser123Ala/Glu143Ala were all obtained using conditions previously found to be successful with HCHL produced using the older plasmid construct pIF1009 [17]. Briefly, crystals were obtained with the hanging-drop vapour diffusion method using a protein concentration of 10 mg mL<sup>-1</sup> in 11% (w/v) PEG 20 000 Da with 8% (v/v) PEG 550 Da monomethyl ether, 0.8 M sodium formate and 0.2% (v/v) butane 1,4-diol in 0.05 M 2-(*N*-morpholino)ethanesulfonic acid buffer pH 5.6. Crystals were routinely flash-cooled in the crystallisation solution. In order to obtain complexes of the mutants with feruloyl-CoA, the proteins were incubated with 10 mM of the substrate for 30 minutes prior to setting up crystal trays.

#### *Data Collection and Data Processing*

Data were collected on a number of crystals that had been complexed with feruloyl-CoA, including the wild-type HCHL, the Ser123Ala mutant, and the Glu143Ala mutant and Ser123Ala/Glu143Ala double mutant. The data collected on both the Glu143Ala and Ser123Ala/Glu143Ala mutants led to electron density maps with ambiguous density in the active site, possibly as a result of their having what was believed to be the significant catalytic residue, Glu-143, removed. The wild-type and Ser123Ala mutants, in contrast, gave rise to good quality electron density maps, and form the basis of the results and discussion below. For the wild-type, data were collected to 2.5Å in-house on a Rigaku Micromax-007HF fitted with Osmic multilayer optics and using a MARRESEARCH MAR345 imaging plate detector. For the Ser123Ala mutant, data were collected to 1.95 Å on beamline ID-144 at the European Synchrotron Radiation Facility, Grenoble. Data were processed and scaled using the interactive HKL2000 suite of programmes [20]. Data collection, processing and refinement statistics for these data sets are presented in Table 3.

#### *Structure Solution and Refinement*

The structures of HCHL and the S123A mutant crystallised with feruloyl-CoA were solved by molecular replacement using the program MOLREP [21] in the interactive suite of programs provided by CCP4 [22] with a monomer of the wild-type HCHL (pdb accession code 2j5i) as the starting model. In the cases of both the wild-type HCHL and the Ser123Ala mutant, the solutions contained six monomers in the asymmetric unit in the form of a hexamer. Following molecular replacement, initial refinement was

performed using the CCP4 program REFMAC5 [23]. Rigid body refinement was performed for 10 cycles. During the refinement process 5% of the data were randomly selected and excluded from refinement for  $R_{\text{free}}$  cross validation. The model was then subjected to positional refinement and initial maximum likelihood weighted  $2Fo-Fc$  and  $Fo-Fc$  maps were calculated. The model was adjusted to fit the electron density maps using the molecular graphics program Coot [24]. Water structure was built into the model using the CCP4 program ARP\_WATERS in ARP/wARP version 5.0 [25], followed by more rounds of positional refinement. In both WT and Ser123Ala structures electron density was present that corresponded to acetyl-CoA. Additional density was also observed near the acetyl terminus of acetyl-CoA, most strongly between subunits *D* and *E* of both WT and Ser123Ala mutant. Only after the building and refinement of waters was acetyl-Coenzyme A added and refined in subunits *B*, *D*, *E*, and *F* of the wild-type HCHL complex and subunits *A*, *B*, *D*, *E*, and *F* of the Ser123Ala mutant. Residual density between subunits Tyr-75 in subunit *D* and Tyr-239 in subunit *E* of both WT and the Ser123Ala mutant was modelled as vanillin, and refined with all atoms set at an occupancy of 1.0, except CAE in the aromatic ring, and the oxygen and methyl of the methoxy group, which were set at an occupancy of 0.5 in both structures. Library files for acetyl-Coenzyme A and vanillin for use in REFMAC5 were created using the PRODRG server [26]. After refinement, the structures were validated using PROCHECK [28]. The refinement statistics of the final models are given in Table 3. In the Ramachandran plot for the WT complex, 91.9% residues were in the most favoured regions, 7.6% in additional allowed regions and 0.5% in generously allowed regions. In the Ser123Ala complex, these values were 93.3%, 6.4% and 0.3% respectively. The atomic coordinates for the WT HCHL and the Ser123Ala mutant, both in complex with acetyl-CoA and vanillin, have been deposited with the Protein databank with the accession numbers 2vss and 2vsu respectively.

## Results and Discussion

### *Cloning and Expression of Genes encoding HCHL and site-directed mutants and determination of kinetic constants.*

For this study, the gene encoding HCHL was re-amplified by PCR from the genomic DNA of *Pseudomonas fluorescens* AN103 and cloned into a new vector construct that allowed isolation of the wild-type enzyme and mutant variants using nickel affinity chromatography. Levels of expression of the HCHL gene were much improved using the new constructs. Recombinant HCHL, mutants Ser123Ala, Glu143Ala, a double mutant, Ser123Ala/Glu143Ala and Tyr239Phe were constructed, and proteins purified from the relevant expression strains. The wild-type HCHL and four mutants were assessed by a UV spectrophotometric kinetic assay based on that used by Mitra and co-workers [8], which monitored the disappearance of feruloyl-CoA at 400 nm. Prior to the synthesis and use of feruloyl-CoA as a substrate, the possibility of using an *N*-acetyl cysteamide derivative was investigated, as such compounds have been shown to be effective and cheaper substrate surrogates for enzymes that use coenzyme-A-ligated substrates [28]. While the synthesis of the *N*-acetylcysteamide of ferulic acid was successful, this substrate analogue proved not to be converted to vanillin by HCHL (results not shown); a result which seems to be explicable by the structural observations contained herein.

The results of the kinetic assays are shown in Table 4. Kinetic constants for the recombinant HCHL with ferulic acid as substrate are of the same order as those obtained by Mitra with the enzyme from *P. fluorescens* if higher in each case. The  $k_{\text{cat}}$  value obtained was  $3.72 \text{ s}^{-1}$  compared to  $1.15 \text{ s}^{-1}$ , and the  $K_{\text{M}}$   $11.8 \text{ }\mu\text{mol}$  compared to  $2.4 \text{ }\mu\text{mol}$ . Mutation of Glu-143 to Ala, either in the single point mutant Glu143Ala or the double mutant Ser123Ala/Glu143Ala resulted in variants for which no activity could be detected at a range of concentrations used in the assays. These results would appear at first glance to confirm that Glu-143 is essential to the mechanism of HCHL activity. Mutation of Ser-123 to Ala resulted in a mutant displaying a reduced  $k_{\text{cat}}$  compared to the wild-type, but not markedly so, and a  $K_{\text{M}}$  comparable to that of the wild-type, suggesting that there is little contribution of this residue to

mechanism or substrate binding. The mutation of Tyr-239 to phenylalanine resulted in a mutant of increased  $K_M$  however, in line with its anticipated role in substrate binding, with a  $K_M$  approximately tenfold higher than that of the wild-type. The mutant retained a significant amount of catalytic activity however, with a  $k_{cat}$  approximately ten times less than that of the wild-type, indicating that the phenolic hydroxyl of Tyr-239 is not absolutely essential for activity. The significance of the data arising from the kinetic analysis of the mutants is discussed below, in the context of the structural data.

#### *Structural studies of WT-HCHL and S123A mutant crystallized with feruloyl-CoA*

In an attempt to acquire a *holo*-HCHL structure four of the variants (WT, Ser123Ala, Glu143Ala and Ser123Ala/Glu143Ala) were crystallized in the presence of the substrate, feruloyl-CoA. Good quality datasets were collected on all crystal complexes, but electron density within the active sites of the Glu-Ala mutants was ambiguous. The wild-type and Ser123Ala structures were very similar in respect of ligand binding characteristics, but the Ser123Ala was the superior dataset, being solved to a resolution of 1.90 Ångstroms. Hence whilst the data for both WT and Ser123Ala complexes are presented and have been deposited (Table 3), the observations described below are derived from the Ser123Ala structure.

The structure of the Ser123Ala mutant complex features only six monomers in the asymmetric unit as contrasted with twelve in the asymmetric unit of *apo*-HCHL [17]. It is notable that of the six monomers in the hexamer, formed of two trimers, the quality of the electron density is not uniform throughout the structure. The poorest density occurs in the helical region of Glu-74 to Ala-81 and corresponds to a flexible helix that is structurally homologous to those in other members of the crotonase superfamily that have themselves been difficult to build. Indeed, in subunit *A*, residues 75 to 80 could not be modelled, and in subunits *B* and *C* the side chain density is poor in some cases. However the density within the trimer that consists of subunits *D*, *E*, and *F* is much better overall, and that between neighbouring monomers *D* and *F* is excellent with respect to density of side chains within an active site that will help describe the loop motions that occur on substrate binding, as it was thought that the substrate binding site for feruloyl-CoA was formed at the monomer-monomer interface in the model built previously [17]. Indeed, ligand density corresponding to some or all of the relevant ligands was observed within five of the six putative active sites of the Ser123Ala mutant. Specifically, clear density for Coenzyme-A was observed that corresponded to the ADP moiety and the pantothenate up to CBX1 in at the interface between monomers *A* and *B* and *D* and *E*. Clear density was also observed for the acetyl portion of acetyl-CoA with the C=O bound, as expected, within an oxyanion hole formed by the peptidic N-Hs of residues Met-70 and Gly-120 at these sites. Between subunit *B* and *C*, *E* and *F*, and *F* and *D*, density corresponding to the complete acetyl-CoA molecule was observed. Between subunit *C* and *A*, there was no electron density for Coenzyme-A.

Acetyl-CoA is bound within the active site of HCHL in a characteristic bent conformation in which the adenine ring binds to the accessible surface of the protein and then wraps round to protrude the pantothenyl chain into the interior of the protein at the dimer interface. Ac-CoA makes a series of non-covalent contacts with the HCHL structure. The amino group of the adenine ring is hydrogen-bonded to the carbonyl group of Met-70. In this respect the binding of Coenzyme A to HCHL is conserved from ECH [18] – the interaction is with the C=O group of the residue whose adjacent peptidic N-H group forms part of the oxyanion hole for enolate binding; the phosphate on the 2' OH of ribose is bonded to Arg-29 (*A*); the diphosphate of ADP is bound by Arg-30 (*A*); the C=O group of the pantothenyl peptide bond closest to sulphur is H-bonded to the side chain hydroxyl of Ser-142; the adjacent N-H is bound by the backbone carbonyl of Ala-88. Whilst density corresponding to the acyl portion of acetyl-CoA was well defined in five out of six active sites, the sulfur atom that is part of the thioester bond, and that completes the continuous density between pantothenate CBX1 and the acetyl group, was only well-defined in three subunits. Processing a truncated dataset (200 images instead of the full data set of



300), at the expense of completeness of the data, suggested that the sulfur was subject to radiation damage.

The poor quality of electron density in the 74-81 helical region of each monomer may in part be attributed to the flexibility of this helix, as has been observed with crotonase homologs CarB [15], menB [29] and enoyl-CoA hydratase [14] itself. An overlap of monomers *A* and *B* from *apo*-HCHL and subunits *D* and *E* of the Ser123Ala mutant reveals the extent of the helix movement on substrate binding. This is illustrated in Figure 4. In ligand-bound HCHL, the helix closes the gap between the two subunits contributing to the active site, and results in marked changes to the positions and orientations of residues therein, notably Met-70, Leu-72, Phe-76 and Tyr-75. Trp-146 and Ile-148 also move on the opposite face of the cavity. Arg-30, which, on the *apo*-form of the enzyme occludes the entrance to the active site, moves to accommodate the Co-A molecule. The most significant consequence of the movement of this helix is the movement of the side chain of Tyr-75 (Figure 3). In *apo*-HCHL, Tyr-75 is hydrogen bonded through its phenolic hydroxyl to the terminal amide of Gln-87, but on substrate binding, this H-bond is broken and the plane of the tyrosine side chain moves a distance of approximately 4 Å into the active site cavity, where it now moves to a distance of 3.6 Å from the phenolic hydroxyl of Tyr-239 on the neighbouring monomer.

On examination of the difference maps in the cavity in the active site between the 'pincer' formed by the phenolic hydroxyls of Tyr-75(*D*) and Tyr-239(*E*) and the terminus of acetyl-CoA, substantial peaks of extra electron density were observed. Continuous electron density was observed between density within H-bonding distance of Glu-143 and to the density within H-bonding distance of the two tyrosine hydroxyls. The density from the omit map at a level of  $3\sigma$  is shown in Figure 5. Vanillin was modelled into this density, with occupancies for all atoms set at 1.0, save the *O*-methyl substitution and one ring carbon, which were set at 0.5. This ligand was refined with no appreciable increase in negative density in the resultant difference map. The phenolic hydroxyl of the vanillin molecule was held between the hydroxyls of the tyrosine pincer at a distance of 2.6 Å from Tyr-75 (*D*) and 2.6 Å Tyr-239 (*E*) (Figure 5). The aldehyde of vanillin was within hydrogen bonding distance of Glu-143 and superimposed with a water molecule that was hydrogen-bonded to Glu-143 in the *apo*-HCHL structure. The carbon atom of the aldehyde was 2.7 Å from the terminal carbon of acetyl-CoA.

The results from the kinetics study and the structures of the WT HCHL and the Ser123Ala mutant complexes appear to uphold some of the hypotheses formulated using the model previously described, as well as revealing unexpected new observations that may help guide further experiments designed to illuminate the mechanism of the enzyme. The reaction catalysed by enoyl-CoA hydratase provides a basis for describing the initial part of the mechanism of hydration of feruloyl-CoA catalysed by HCHL. In ECH, it was proposed that a water molecule, stabilized by interactions with Glu-144 and Glu-164, is that which is activated for hydration of the double bond by means of a concerted E1cB mechanism [18]. In native HCHL, such a water molecule is bound by the side chain of Glu-143 (the homolog of Glu-164<sub>ECH</sub>) and the backbone N-H of Gly-151. In a postulated mechanism for HCHL activity based on the ECH mechanism, the oxygen atom from the water that attacks the benzylic position would become the oxygen of the aldehyde of the vanillin molecule following C-C bond cleavage. In fact, when *apo*-HCHL and the *holo*-Ser123Ala structures are superimposed, the water adjacent to Glu-143 in the *apo*-enzyme and the oxygen of the aldehyde group are superimposed, providing excellent evidence for the role of Glu-143 as the catalytic base primarily responsible for water activation in HCHL, in conjunction with the kinetic analysis of Glu143Ala and Ser123Ala/Glu143Ala, which exhibit no measurable activity against feruloyl-CoA.

Although sequence alignments of ECH and HCHL suggested that Ser-123 may have been a residue of possible catalytic significance within HCHL, both structural and kinetics analysis of WT HCHL in comparison with the Ser123Ala mutant suggest that this residue has a peripheral role. In the WT HCHL

complex structure, the side-chain hydroxyl of Ser-123 is located 6.4 and 8.7 Å from the terminal carbon atoms of vanillin and acetyl-CoA respectively, making it very unlikely that this residue is involved in C-C bond cleavage. In fact, in both *apo*-WT-HCHL and the *holo*-HCHL, Ser-123 appears to have a role in maintaining the active site topology, forming a pocket for the binding of a water molecule in conjunction with the side chain of Gln-98 and the backbone carbonyl of Gly-120, although this water molecule is still present in the Ser123Ala mutant and is approximately 3.9 Å from CAG atom in the aromatic ring of vanillin in both WT and Ser123Ala structures. The peripheral role of Ser123Ala suggested by structure is also evidenced by the kinetics: the  $K_M$  for feruloyl-CoA is comparable to that of the WT and the  $k_{cat}$  is decreased only fourfold. The interest in Ser-123 stemmed from both its presence as the direct sequence homolog of Glu-144 (ECH), coupled with recent observations of serine as a catalytic residue for the cleavage of C-C bonds in *meta*-cleavage product (MCP) hydrolases, in which it has been suggested to act either as a nucleophile [30] or as a general base for the formation of a *gem*-diol intermediate [31]. However, it is clear from the structural studies that the serine is in no way part of a catalytic triad and is too distant from the site of reaction to be catalytically relevant to C-C bond cleavage in either of these modes. The history of study of the crotonase superfamily has suggested that it is difficult to impute catalytic significance to residues on the basis of sequence homology alone, particularly when two different crotonase homologs may catalyse very different chemical reactions [9]. Of carbon-carbon bond cleaving reactions in the crotonase superfamily, neither methylmalonyl decarboxylase (MMDC) [13], 2-ketocyclohexanecarboxyl-CoA hydrolase [11] or 6-oxo camphor hydrolase [37] is as yet known to employ a serine in C-C bond cleavage. MMDC employs a tyrosine residue in the decarboxylation of its substrate, but this shares neither sequence nor structural context with the tyrosines in the active site of HCHL. It is believed rather that the clues to the mechanism of C-C bond cleavage come more from the three-dimensional conservation of ligand recognition between HCHL and other phenol-processing enzymes, rather than from the one residue alone that might be illustrated by conservation with other crotonases, as described below.

The movement of the flexible helix on substrate binding results in the coming together of the phenolic hydroxyls of Tyr-75 and Tyr-239 of the neighbouring monomer. The electron density observed between these phenolic hydroxyls is consistent with being the aromatic product of C-C bond cleavage, vanillin. This observation immediately sheds light on the experimentally observed substrate specificity of HCHL [8]. Compounds such as caffeoyl-CoA and *p*-coumaroyl-CoA, which bear a *para*-hydroxy group on the aromatic ring are substrates, whereas cinnamoyl-CoA (no *p*-hydroxy group) and syringoyl-CoA (*p*-hydroxy group sterically crowded by adjacent methoxy groups) are not. The relevance of one of these tyrosine residues to substrate recognition is evidenced by the ten-fold increase in  $K_M$  observed when this residue is mutated to Phe. The role of the tyrosine pincer as a molecular determinant of substrate recognition also gives a deeper insight into the evolution of substrate recognition of *para*-hydroxy-coumaric acids in other enzymes. The flavoenzyme vanillyl alcohol oxidase (VAO) from *Penicillium simplicissimum* catalyses the flavin dependent oxidation of *para*-substituted phenols such as 4-(methoxymethyl)phenol [32]. In the first catalytic step, hydride is transferred from the substrate to an active site flavin, to yield a substrate *para*-quinone methide intermediate (Figure 6). The flavin is regenerated by reaction with molecular oxygen, and then a water molecule, activated by Asp-170, attacks the benzylic position of the quinone methide to yield *para*-hydroxybenzaldehyde and methanol [33]. The structure of VAO [32, 34] in complex with the ligand 2-methoxy-4-vinylphenol (pdb entry 1w1k) revealed a tyrosine pincer involved in the recognition of the *para*-hydroxy group of that ligand, similar to that observed with HCHL. A superimposition of the relevant active site residues within the active sites of VAO and HCHL (Figure 7) reveals a startling coincidence of a constellation of active site residues, including the tyrosine phenolic hydroxyls as part of the pincer, but also the arginine residue (Arg-91 in HCHL) that is thought to be important in stabilizing negative charge on the *para*-quinone methide and Glu-143, which activates a water molecule for attack at the benzylic carbon on HCHL, and its structural homolog, Asp-170 in VAO. The coincidence of the tyrosine pincer in HCHL and VAO may be

significant, as the role of these residues and the structurally conserved arginine in VAO is thought to be specifically the deprotonation of the phenolic hydroxyl of 4-(methoxymethyl)phenol and subsequent stabilization of the quinone methide intermediate.

This observation may provide clues as to the overall mechanism of double bond hydration and subsequent C-C bond cleavage in HCHL. Such a mechanism would have to account for the experimental evidence that demonstrates that HMPH-CoA is an intermediate [8] and that Glu-143 is the only acid-base residue within reactive distance of the bond to be hydrated thence cleaved. Given the proposed mechanism for VAO, and the established quinone methide intermediate implicated in the mechanism of 4-hydroxycinnamate decarboxylase (another C-C bond cleaving enzyme that works on a ferulic acid derivative [38]), it seems reasonable to suggest that a quinone methide intermediate may be involved in the HCHL mechanism [Figure 8 – (i)]. In contrast to flavoenzymes such as VAO, HCHL does not need to exploit an electron sink in the form of a flavin as it can displace electron density through to the oxygen of the thioester to form an enolate stabilised in the oxyanion hole conserved amongst most crotonases. In the revised mechanism, deprotonation of the phenolic hydroxyl of feruloyl-CoA would lead to the formation of the quinone-methide-enolate (QME) shown. The QME may be the substrate for hydration by the water molecule activated by Glu143 (shown in (ii)) analogous to the hydration of a quinone methide in the VAO mechanism. Whilst it is difficult to speculate on the exact mechanism of C-C bond cleavage subsequent to hydration at this stage, Glu143, which has already acted as a base in the activation of water, is ideally situated to act both an acid to protonate the double bond, leading to the intermediate HMPHP-CoA (iii), and as a catalytic base to promote the *retro*-aldol reaction (iv), which might also be favoured by strain effects exerted by the binding of the phenolic hydroxyl by Tyr75 and Tyr239. The possible role of a quinone methide intermediate in HCHL catalysis has not been established, but may be addressed in future using stopped-flow kinetics techniques such as those used for the study of VAO [35].

In conclusion, kinetics analysis and structural studies of HCHL complexed with its substrate, feruloyl-CoA, have confirmed the role of Glu-143 in the hydration of the substrate leading to the formation of the products of reaction, acetyl-CoA and vanillin. A subtle helix movement on substrate binding has resulted in an unforeseen convergence of tyrosine residues that appears to be responsible for binding the phenolic hydroxyl of the substrate. These results, together with the observation that significant active site residues of HCHL superimpose with the active site of vanillyl alcohol oxidase, provide a structural basis for previously observed substrate discrimination by HCHL and illustrate a remarkable convergence of the molecular determinants of ligand recognition between two structurally unrelated enzymes.

## Acknowledgement

We thank the Biotechnology and Biosciences Research Council (BBSRC) for funding a studentship (to JPB).

## References

1. Walton, N. J., Mayer, M.J. and Narbad, A. (2003). Vanillin. *Phytochemistry* **63**, 505–515
2. Rosazza, J.P.N., Huang, Z., Dostal, L., Volm, T. and Rousseau, B. (1995) Biocatalytic transformation of ferulic acid: an abundant aromatic natural product. *J. Ind. Microbiol.* **15**, 457-471
3. Muheim, A. and Lerch, K. (1999) Towards a high-yield bioconversion of ferulic acid to vanillin. *Appl. Microbiol. Biotechnol.* **51**, 456–461
4. Overhage, J., Priefert, H. and Steinbüchel, A. (1999) Biochemical and genetic analyses of ferulic acid catabolism in *Pseudomonas* HR199. *Appl. Environ. Microbiol.*, **65**, 4837-4847

5. Plaggenborg, R., Overhage, J., Steinbüchel, A. and Priefert, H. (2004) Functional analyses of genes involved in the metabolism of ferulic acid in *Pseudomonas putida* KT2440 Appl. Microbiol. Biotechnol., **61**, 528-535
6. Narbad, A. and Gasson, M.J. (1998) Metabolism of ferulic acid via vanillin using a novel Co-A dependent pathway in a newly-isolated strain of *Pseudomonas fluorescens*. Microbiology, **144**, 1397-1405
7. Gasson, M.J., Kitamura, Y., McLauchlan, W.R., Narbad, A., Parr, A.J., Parsons, E.H.L., Payne, J., Rhodes, M.J.C. and Walton, N.J. (1998) Metabolism of ferulic acid to vanillin. J. Biol. Chem., **273**, 4163-4170
8. Mitra, A., Kitamura, Y., Gasson, M.J., Narbad, A., Parr, A.J., Payne, J., Rhodes, M.J.C., Sewter, C. and Walton, N.J. (1999) 4-hydroxycinnamoyl-CoA hydratase/lyase (HCHL) - an enzyme of phenylpropanoid chain cleavage from *Pseudomonas*. Arch. Biochem. Biophys. **365**, 10-16.
9. Holden, H.M., Benning, M.M., Haller, T. and Gerlt, J.A. (2001) The crotonase superfamily: divergently related enzymes that catalyze different reactions involving acyl coenzyme A thioesters. Acc. Chem. Res. **34**, 145-157
10. Agnihotri G. and Liu H (2003) Enoyl-CoA hydratase - Reaction, mechanism, and inhibition. *Bioorg. Med. Chem.*, **11**, 9-20
11. Eberhard, E. D. and Gerlt, J. A. (2004) Evolution of Function in the Crotonase Superfamily: The Stereochemical Course of the Reaction Catalyzed by 2-Ketocyclohexanecarboxyl-CoA Hydrolase, J. Am. Chem. Soc., **126**, 7188-7189
12. Benning, M.M., Taylor, K.L. Liu, R-Q. Yang, G., Xiang, H., Wesenberg, G., Dunaway-Mariano, D. and Holden, H.M. (1996) Structure of 4-Chlorobenzoyl Coenzyme A Dehalogenase Determined to 1.8 Å Resolution: An Enzyme Catalyst Generated via Adaptive Mutation. *Biochemistry* **35**, 8103-8109
13. Benning, M. M., Haller, T., Gerlt, J. A. & Holden, H. M. (2000) New Reactions in the Crotonase Superfamily: Structure of Methylmalonyl CoA Decarboxylase from *Escherichia coli*. *Biochemistry*, **39**, 4630-4639
14. Engel, C.K., Mathieu, M., Zeelen, J. Ph. Hiltunen, J.K. and Wierenga, R.K. (1996) Crystal structure of enoyl-coenzyme A (CoA) hydratase at 2.5 Ångstroms resolution: a spiral fold defines the CoA-binding pocket. *EMBO J.* **15**, 5135-5145
15. Sleeman, M.C., Sorensen, J.L., Batchelar, E.T., McDonough, M.A. and Christopher J. Schofield (2005) Structural and Mechanistic Studies on Carboxymethylproline Synthase (CarB), a Unique Member of the Crotonase Superfamily Catalyzing the First Step in Carbapenem Biosynthesis. *J. Biol. Chem.* **280**, 34956-34965
16. Widboom, P.F., Fielding, E. N., Liu, Y. and Bruner, S.D. (2007) Structural basis for cofactor-independent dioxygenation in vancomycin biosynthesis. *Nature* **447**, 342-345.
17. Leonard, P. M., Brzozowski, A. M., Lebedev, A., Marshall, C. M., Smith, D. J., Verma, C. S., Walton, N. J. & Grogan, G. (2006) The 1.8 Å resolution structure of hydroxycinnamoyl-coenzyme A hydratase-lyase (HCHL) from *Pseudomonas fluorescens*, an enzyme that catalyses the transformation of feruloyl-coenzyme A to vanillin. *Acta Crystallogr. Sect. D. Biol. Crystallogr.* **62**, 1494-1501

18. Bahnson, B. J., Anderson, V. E. & Petsko, G. A. (2002) Structural Mechanism of Enoyl-CoA Hydratase: Three Atoms from a Single Water Are Added in either an E1cb Stepwise or Concerted Fashion *Biochemistry*, **41**, 2621-2629
19. Bonsor, D., Butz, S.F., Solomons, J., Grant, S.C., Fairlamb, I.J.S., Fogg, M.J. and Grogan, G. (2006) Ligation Independent Cloning (LIC) as a rapid route to families of recombinant biocatalysts from sequenced prokaryotic genomes. *Org. Biomol. Chem.* **4**, 1252-1260
20. Otwinowski, Z and Minor, W. (1997) Processing of X-ray Diffraction Data Collected in Oscillation Mode. *Methods in Enzymology, Macromolecular Crystallography, part A.* **276**, 307-326. Carter, Jr., C.W. and Sweet, R.M. Eds., Academic Press (New York)
21. Vagin, A. and Teplyakov, A. (1997) *MOLREP*: an Automated Program for Molecular Replacement. *J. Appl. Cryst.* **30**, 1022-1025
22. Collaborative Computational Project, Number 4. (1994) *Acta Crystallogr., Sect D: Biol. Crystallogr.*, **50**, 760-763
23. Murshudov, G. N., Vagin, A. A., and Dodson, E. J. (1997) Refinement of Macromolecular Structures by the Maximum-Likelihood Method. *Acta Crystallogr., Sect D: Biol. Crystallogr.*, **53**, 240-255
24. Emsley, P., Cowtan, K. (2004) Coot: model-building tools for molecular graphics. *Acta Crystallogr., Sect D: Biol. Crystallogr.*, **60**, 2126-2132
25. Perrakis, A., Morris, R., and Lamzin, V. S. (1999) Automated protein model building combined with iterative structure refinement. *Nat. Struct. Biol.*, **6**, 458-463
26. Schuettelkopf, A.W. and van Aalten, D.M.F. (2004) PRODRG - a tool for high-throughput crystallography of protein-ligand complexes. *Acta Crystallogr. Sect. D. Biol. Crystallogr.* **60**, 1355-1363
27. Laskowski, R. A., Macarthur, M. W., Moss, D. S., and Thornton, J. M. (1993) PROCHECK: a program to check the stereochemical quality of protein structure coordinates. *J. Appl. Crystallogr.* **26**, 283-291
28. Less, S.L, Handa, S., Millburn, K., Leadlay, P.F., Dutton, C.J. and J. Staunton (1996) Biosynthesis of Tetronasin: Part 6. Preparation of Structural Analogues of the Diketide and Triketide Biosynthetic Precursors to Tetronasin. *Tetrahedron Lett.*, **37**, 3515-3518
29. Johnston, J.M., Arcus, V.L. and Baker, E.N. (2005) Structure of naphthoate synthase (MenB) from *Mycobacterium tuberculosis* in both native and product-bound forms. *Acta Crystallogr. Sect. D. Biol. Crystallogr.* **61**, 1191-1206
30. Horsman, G.P., Bhowmik, S., Seah, S.Y.K., Kumar, P., Bolin, J.T and Eltis, L.D. (2006) The tautomeric Half-reaction of BphD, a C-C Bond Hydrolase. *J. Biol. Chem.* **282**, 19894-19904
31. Li, J.-J.; Li, C., Blindauer, C. A. and Bugg, T. D. H. (2006) Evidence for a *gem*-Diol Reaction Intermediate in Bacterial C-C Hydrolase Enzymes BphD and MhpC from <sup>13</sup>C NMR Spectroscopy. *Biochemistry* **45**, 12461-12469
32. Mattevi, A., Fraaije, M. W., Mozzarelli, A., Olivi, L., Coda, A. and van Berkel, W.J.H. (1997) Crystal structures and inhibitor binding in the octameric flavoenzyme vanillyl-alcohol oxidase: the shape of the active-site cavity controls substrate specificity *Structure*, **5**, 907-920

33. van den Heuvel, R.H.H., Fraaije, M. W., Mattevi, A., van Berkel, W. J.H. (2000) Asp-170 Is Crucial for the Redox Properties of Vanillyl-alcohol Oxidase. *J. Biol. Chem.*, **275**, 14799-14808
34. van den Heuvel, R.H., van den Berg, W.A., Rovida, S. and van Berkel, W.J. (2004) Laboratory-evolved vanillyl-alcohol oxidase produces natural vanillin. *J.Biol.Chem.* **279**, 33492-33500
35. Fraaije, M.W. and van Berkel W.J.H. (1997) Catalytic Mechanism of the Oxidative Demethylation of 4-(Methoxymethyl)phenol by Vanillyl Alcohol Oxidase. Evidence for Formation of a *p*-Quinone Methide Intermediate. *J. Biol. Chem.*, **272**, 18111-18116
36. Wu, W-J., Tonge, P.J. and Raleigh D.P. (1998) Stereospecific  $^1\text{H}$  and  $^{13}\text{C}$  NMR Assignments of Crotonyl CoA and Hexadienoyl CoA: Conformational Analysis and Comparison with Protein-CoA Complexes. *J. Am. Chem. Soc.* **120**, 9988-9994
37. Leonard, P.M. and Grogan G. (2004) Structure of 6-Oxo Camphor Hydrolase H122A Mutant Bound to Its Natural Product, (2*S*, 4*S*)- $\alpha$  -Campholinic Acid. *J. Biol. Chem.* **279**, 31312-31317.
38. Hashidoko, Y. and Tahara, S. (1998) Stereochemically Specific Proton Transfer in Decarboxylation of 4-Hydroxycinnamic acids by 4-Hydroxycinnamate Decarboxylase from *Klebsiella oxytoca*. *Arch. Biochem. Biophys.* **359**, 225-230.

Table 1.  $^1\text{H}$  NMR spectroscopic data for feruloyl-S-CoA.

Attribute	$\delta$ (ppm)	Multiplicity	$J$ / Hz
2- <i>H</i>	8.01	s	-
8- <i>H</i>	8.36	s	-
1'- <i>H</i>	5.96	d	6.3
2'- <i>H</i>	<sup>a</sup>	-	-
3'- <i>H</i>	<sup>a</sup>	-	-
4'- <i>H</i>	4.50	br s	-
5'- $\text{CH}_2$	4.20	br s	-
1''- $H_a$	3.53 ( <i>pro-S</i> ) <sup>b</sup>	dd	4.5, 9.7
1''- $H_b$	3.81 <sup>c</sup> ( <i>pro-R</i> ) <sup>b</sup>	m	-
3''- <i>H</i>	3.99	s	-
5''- $H_2$	3.42	m	-
6''- $H_2$	2.42	t	6.2
8''- $H_2$	3.37	t	5.9
9''- $H_2$	3.07	m	-
10''- $\text{CH}_3$	0.87 ( <i>pro-R</i> ) <sup>b</sup>	s	-
11''- $\text{CH}_3$	0.73 ( <i>pro-S</i> ) <sup>b</sup>	s	-
2 <sup>a</sup> - <i>H</i>	6.45	d	15.7
3 <sup>a</sup> - <i>H</i>	7.23	d	15.7
5 <sup>a</sup> - <i>H</i>	6.89	s	-
8 <sup>a</sup> - <i>H</i>	6.74	d	8.1
9 <sup>a</sup> - <i>H</i>	6.87	d	8.1
10 <sup>a</sup> - $\text{OCH}_3$	3.77 <sup>d</sup>	s	-

<sup>a</sup> Proton signals overlapping with residual  $\text{H}_2\text{O}$  signal.

<sup>b</sup> Stereochemistry tentatively assigned by comparison with the reported data [36].

<sup>c</sup> Overlapping signal with 10<sup>a</sup>- $\text{OCH}_3$  and trace impurity.

<sup>d</sup> Overlapping signal with 1''- $H_b$  and trace impurity.

Table 2. Primers used for PCR in amplification of gene encoding HCHL from genomic DNA of *P. fluorescens* AN1003 and subsequent site-directed mutagenesis experiments.

Variant	Template	Forward Primer	Reverse Primer
WT	Genomic DNA	CCAGGGACCAGCAATGAG CACATACGAAGGTCGCTG GAAAAC	GAGGAGAAGGCGCGTTAT CAGCGTTTATACGCTTGCA GGCCAG
Ser123Ala	pLB001	TGCTTCGGCGGGCGGTTTC GCCCCGCTGGTGGCCTGC GAC	GTCGCAGGCCACCAGCGG GGCGAAACCGCCCGCGAA GCA
Glu143Ala	pLB001	GCAACCTTCGGTCTCTCG GCCATCAACTGGGGTATC CCG	CGGGATACCCAGTTGAT GGCCGAGAGACCGAAGGT TGC
Tyr239Phe	PLB001	CAG AAC GAG GAT TAC CTG TTC GCC AAG CTC GAT CAG TCG	CGA CTG ATC GAG CTT GCG GAA CAG GTA ATC CTC GTG CTG
Ser123Ala/Glu143Ala	pLB002	As for Glu143Ala	



	WT-HCHL complex with acetyl-CoA/vanillin	Ser123Ala mutant complex with acetyl-CoA/vanillin
Beamline	Rigaku Micromax-007HF (in-house)	ID-144 (ESRF)
Wavelength (Å)	1.54178	0.93950
Resolution (Å)	97.13-2.22 (2.27-2.22)	96.67-1.90 (1.95-1.90)
Space Group	$P2_12_12_1$	$P2_12_12_1$
Unit cell (Å)	90.2, 130.6, 144.6	90.1, 130.1, 144.7
Unique reflections	73967 (2976)	123802 (7182)
Completeness (%)	91.5 (50.3)	96.7 (76.8)
$R_{\text{sym}}$ (%)	12 (32)	10 (69)
Multiplicity	5.2 (4.7)	5.5 (2.9)
$\langle I/\sigma(I) \rangle$	9.0 (2.9)	6.8 (2.5)
Protein atoms	11517	11690
Solvent waters	313	488
$R_{\text{cryst}}/R_{\text{free}}$	0.18/0.24	0.19/0.23
r.m.s.d 1-2 bonds (Å)	0.023	0.017
r.m.s.d 1-3 angles (°)	1.966	1.635
Chiral centre (Å <sup>3</sup> )	0.124	0.109
Planarity	0.008	0.007
Avge main chain B (Å <sup>2</sup> )	37	25
Avge side chain B (Å <sup>2</sup> )	37	24
Avge solvent B (Å <sup>2</sup> )	36	27
Avge ligand B ( Å <sup>2</sup> , Coenzyme-A)	35	31
Avge ligand B ( Å <sup>2</sup> , Vanillin)	42	30

Table 3. Data collection and refinement statistics for WT-HCHL and S123A mutant co-crystallised with feruloyl-CoA. Values in parentheses refer to the highest resolution shell. Values in square brackets are target values.  $R_{\text{sym}} = \frac{\sum_{\mathbf{h}} \sum_l |I_{\mathbf{h}l} - \langle I_{\mathbf{h}} \rangle|}{\sum_{\mathbf{h}} \sum_l \langle I_{\mathbf{h}} \rangle}$ , where  $I_l$  is the  $l$ th observation of reflection  $\mathbf{h}$  and  $\langle I_{\mathbf{h}} \rangle$  is the weighted average intensity for all observations  $l$  of reflection  $\mathbf{h}$ .  $\langle I/\sigma(I) \rangle$  indicates the average of the intensity divided by its S.D.

Table 4. Kinetic parameters determined for HCHL and mutants using feruloyl-CoA as substrate

HCHL variant	$K_M$ (mol dm <sup>-3</sup> x 10 <sup>-3</sup> )	$k_{cat}$ (s <sup>-1</sup> )	$k_{cat}/K_M$ (mol <sup>-1</sup> dm <sup>3</sup> s <sup>-1</sup> x 10 <sup>4</sup> )
Wild-type	0.0118 ± 0.002	3.72 ± 0.18	31.52
Ser123Ala	0.0135 ± 0.002	0.96 ± 0.03	7.11
Glu143Ala	n.d.	n.d.	-
Ser123Ala/Glu143Ala	n.d.	n.d.	-
Tyr239Phe	0.095 ± 0.020	0.41 ± 0.06	0.43

## Figure Legends

Figure 1. Biotransformation of ferulic acid **1** to vanillin **4** by *Pseudomonas fluorescens* AN103.

Figure 2. Sequence homology of HCHL and enoyl-CoA hydratase (ECH) in the region of the major catalytic residues of ECH. The triglycine motif is underlined. The central glycine of the GGG motif contributes one of the peptidic N-Hs for the formation of the oxyanion hole conserved amongst crotonase homologs.

Figure 3.  $^{31}\text{P}\{^1\text{H}\}$  NMR spectrum (202 MHz) of feruloyl-SCoA [14 mM] in  $\text{D}_2\text{O}$  at 300 K. The  $^2J_{\text{P}\alpha\text{P}\beta}$  spin-spin coupling was confirmed by a 2D  $^{31}\text{P}$ - $^{31}\text{P}$  COSY experiment.

Figure 4. Helix movement undergone by HCHL upon substrate binding, as observed in the structure of the Ser123Ala mutant co-crystallised with feruloyl-CoA. The backbone of the native structure is shown in dark grey and the *holo*-enzyme (Ser123Ala) is shown in light green. A hydrogen bond (dashed) between Gln-87 and Tyr-75 is broken when the substrate binds and Tyr-75 moves upwards into the active site (shown by the arrow). In this new position, Tyr-75 comes into close contact with Tyr-239 from the neighbouring monomer. Also shown is acetyl-Coenzyme A with the adenine  $-\text{NH}_2$  hydrogen bonded to the backbone carbonyl of Met-70, and its movement on substrate binding.

Figure 5. Dimer interface on the Ser123Ala mutant of HCHL, complexed with vanillin and acetyl-CoA. Subunit (*D*) is shown in light grey; subunit (*E*) in dark grey. Residual electron density was observed in the difference maps after building and refining protein, water and acetyl-CoA structures. Vanillin has been built into this density, which corresponds to the  $2F_o - F_c$  electron density map contoured at  $3\sigma$  level *before* refinement of the ligand. For purposes of refinement, all occupancies were set to a level of 1.0, except the CAE of the aromatic ring and the methoxy group, which were set at 0.5. The phenolic hydroxyl of vanillin can be seen occupying space at hydrogen bonding distance to both Tyr-75 (*D*) and Tyr-239 (*E*). The aldehyde of vanillin is within H-bonding distance of the side chain of Glu-143. These H-bonding interactions are indicated by black dashed lines.

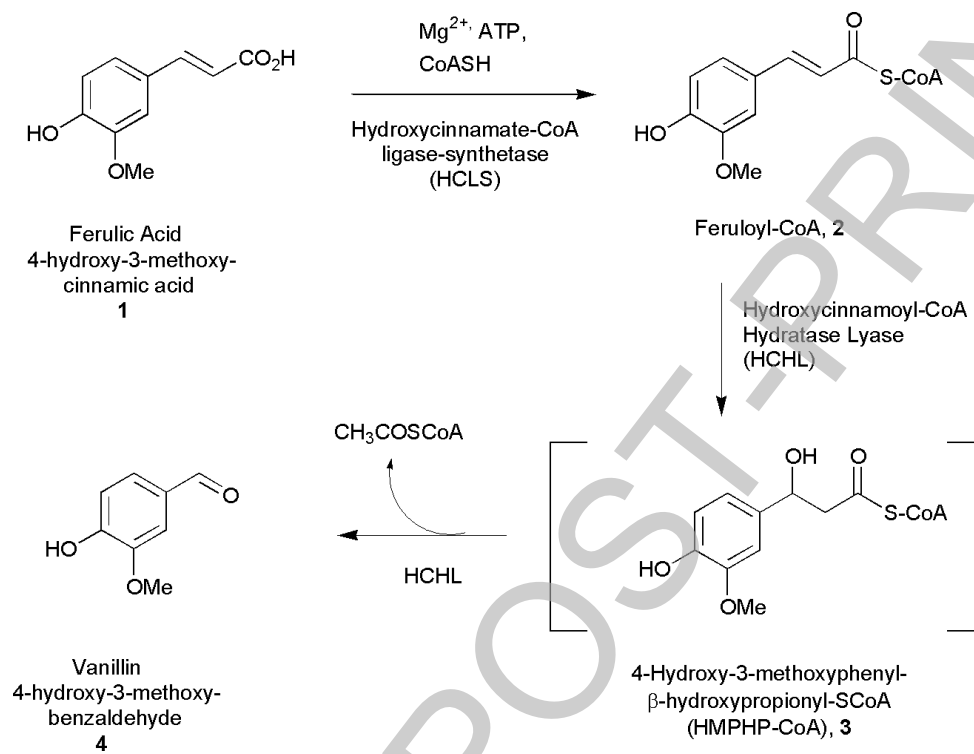
Figure 6. Partial mechanism of vanillyl alcohol oxidase (VAO, derived from reference [33]) showing formation of quinone methide intermediate initiated by deprotonation of the substrate phenolic hydroxyl by two tyrosine residues and transfer of hydride to flavin. Asp-170 shown was also thought to act as a catalytic base for the activation of a water molecule for hydration of the double bond of the quinone methide.

Figure 7. Superimposition of a constellation of active site residues in HCHL (shown with side-chain carbon atoms and labels in dark grey) and vanillyl alcohol oxidase (VAO from pdb entry 1w1k, side chain carbon atoms and labels in light grey). Superimposition was generated in the program ccp4mg (38) by overlaying the hydroxyls of the tyrosine residues and the phenolic hydroxyls of vanillin (carbon atoms in grey) and 2-methoxy-4-vinylphenol, the VAO ligand (carbon atoms in dark green).

Figure 8. Proposed mechanism for HCHL-catalysed transformation based on structural observations. (i) Tyr75 (*D*) and Tyr239 (*E*) initiate deprotonation of the phenolic hydroxyl of feruloyl-CoA, leading to a quinone-methide-enolate (QME) that is stabilized in the oxyanion hole conserved in most crotonase homologs. The QME is hydrated (ii) and Glu143 donates a proton to form HMPHP-CoA (3, Figure 1). Intramolecular proton transfer (iv) yields acetyl CoA and vanillin as the final products.

Stage 2(a) POST-PRINT

**Figure 1**



THIS IS NOT THE FINAL VERSION - see doi:10.1042/BJ20080714

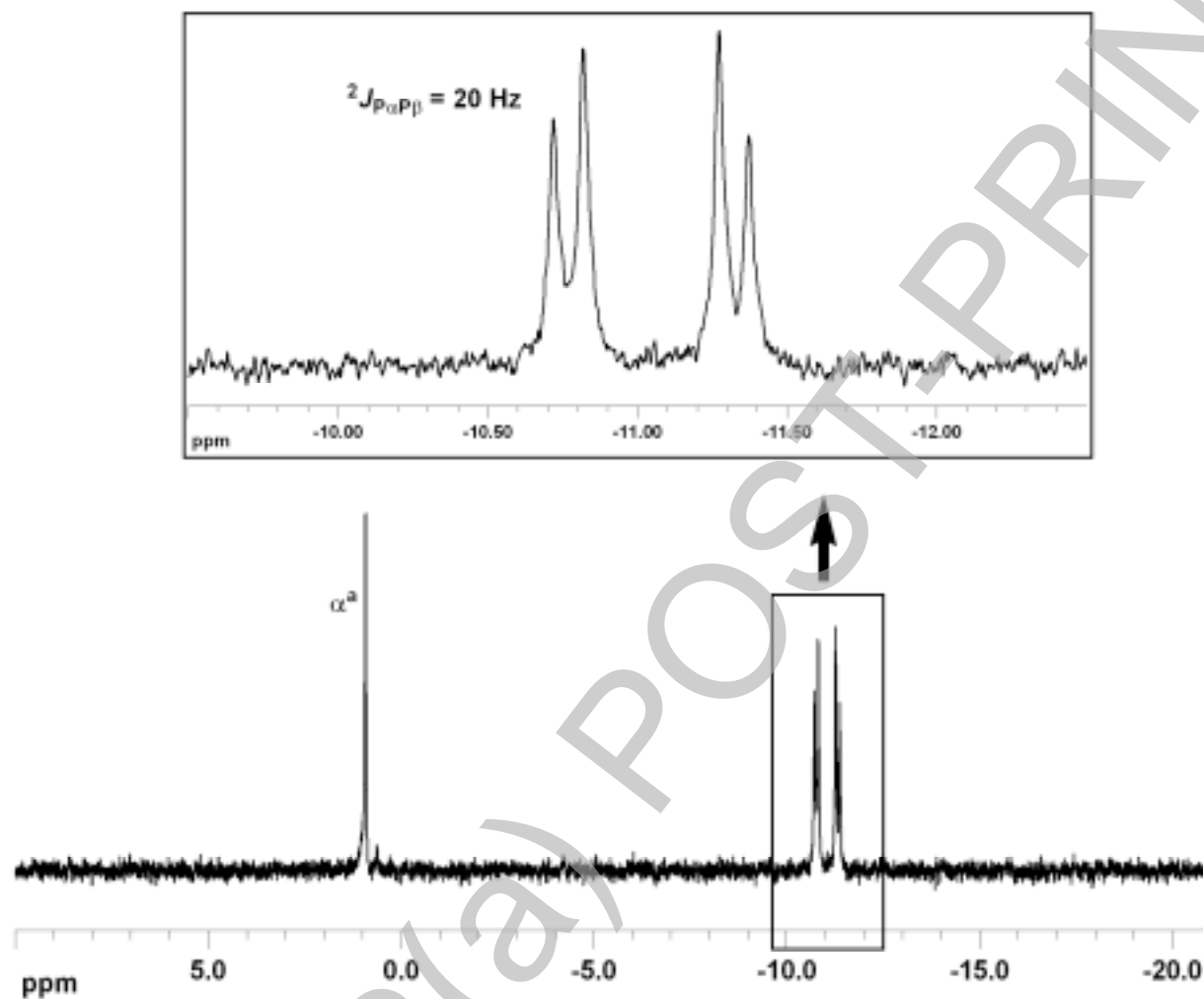
**Figure 2**

	<b>ECH Glu-144</b>	<b>ECH Glu-164</b>
ECH	PVIAAVNGYAL <u>GGG</u> CELAMMCDIIYAGEKAQFGQPEI LLGTIPGA 173	
HCHL	PTIAMVNGWCF <u>GGG</u> FSLVACDLAICADEATFGLSEINWGIPPGN 152	
	*. ** *** : . : *** . : ** : . . . : * ** . ** * **	
	<b>HCHL Ser-123</b>	<b>HCHL Glu-143</b>

Stage 2(a) POST-PRINT

THIS IS NOT THE FINAL VERSION - see doi:10.1042/BJ20080714

**Figure 3**



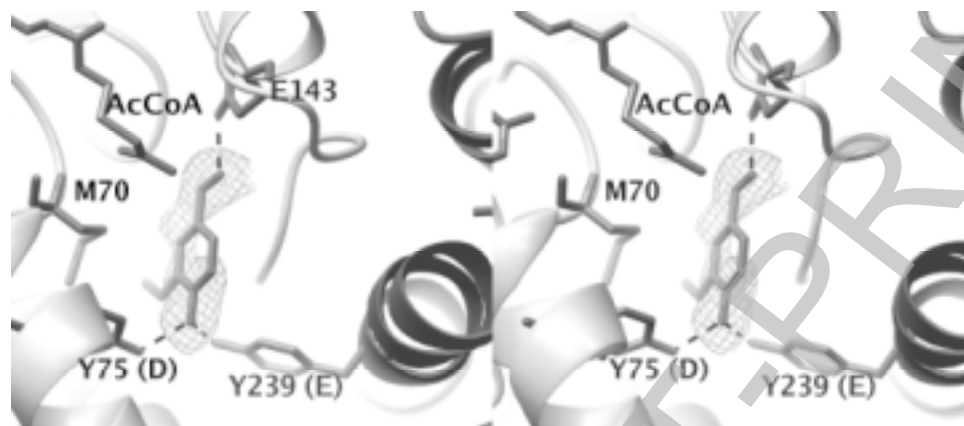
THIS IS NOT THE FINAL VERSION - see doi:10.1042/BJ20080714

Figure 4

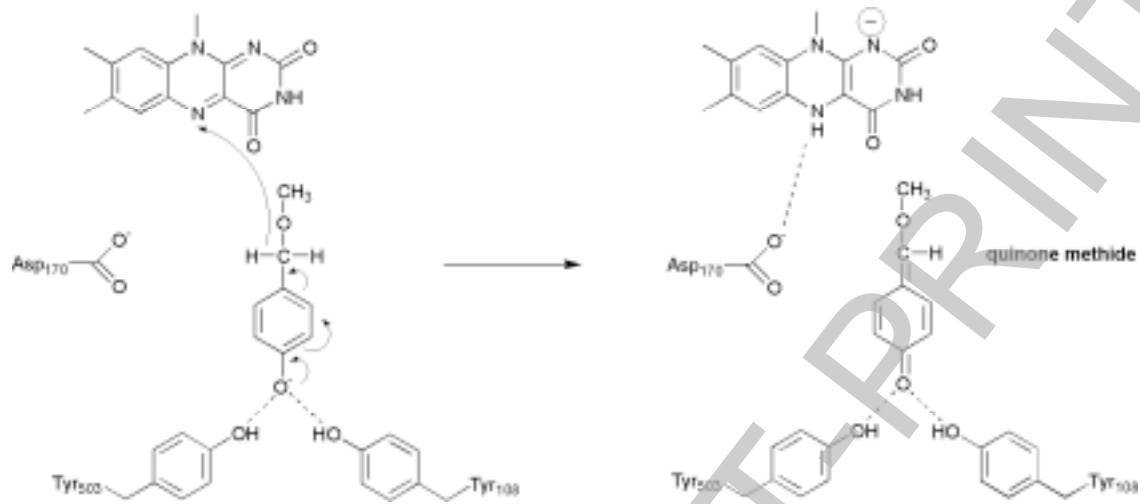




Figure 5



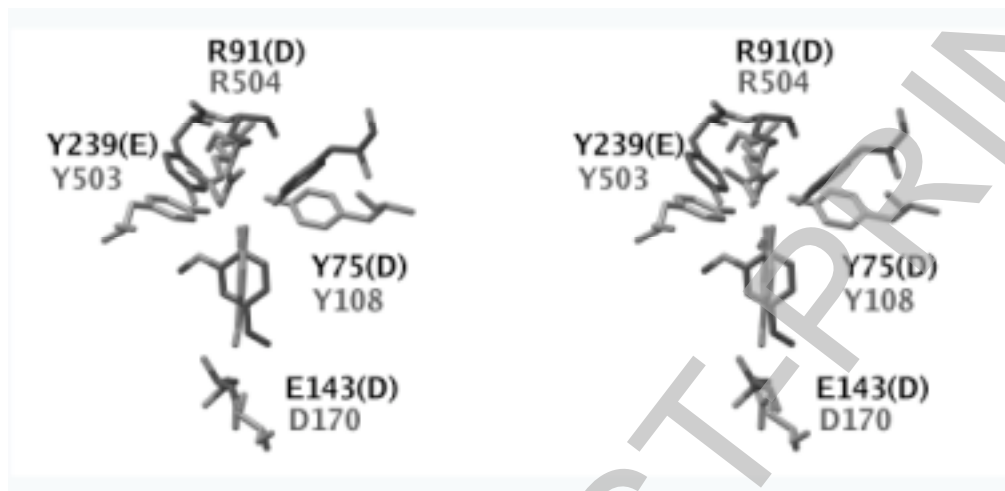
**Figure 6**



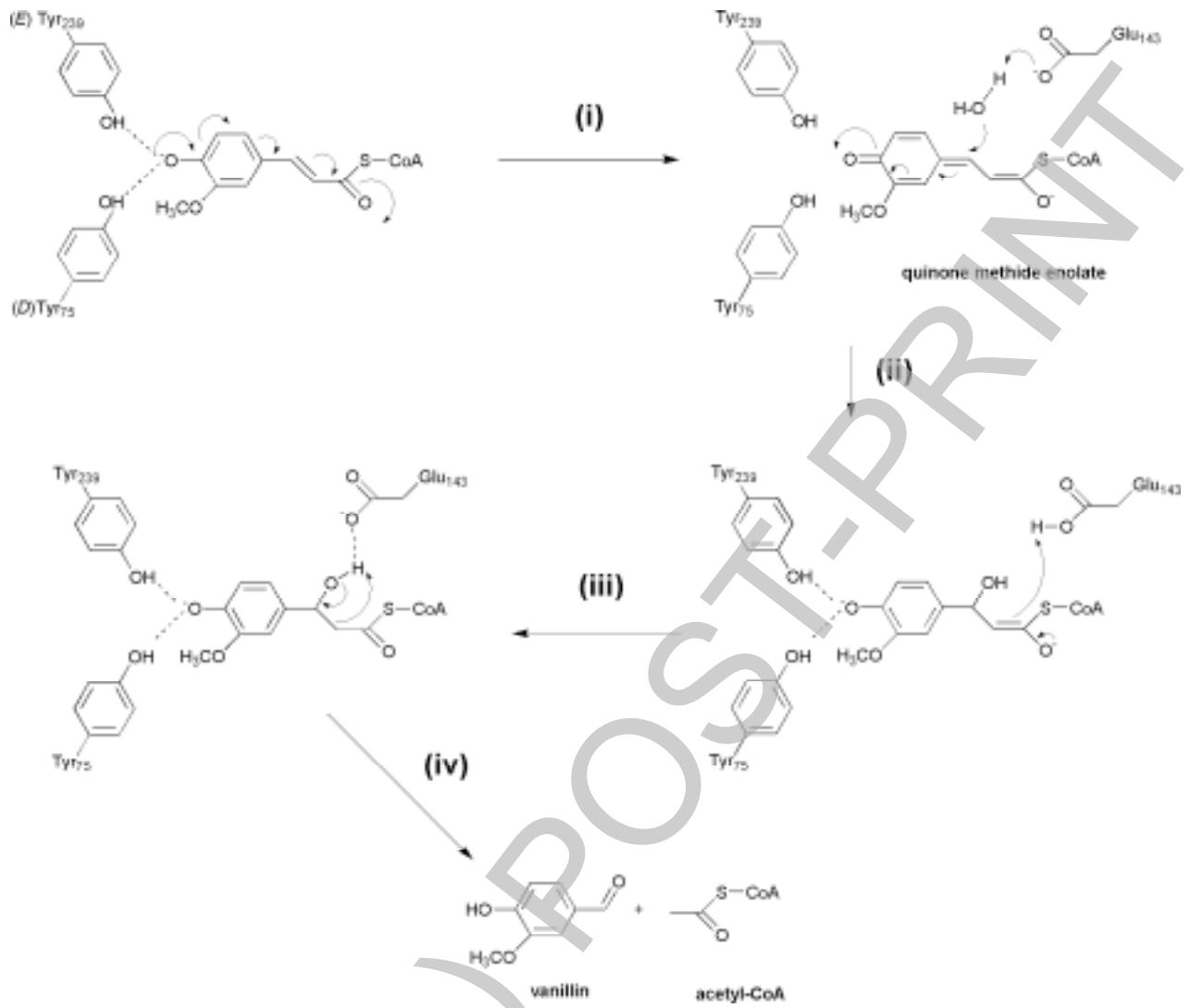
Stage 2(a) POST-PRINT

THIS IS NOT THE FINAL VERSION - see doi:10.1042/BJ20080714

Figure 7



**Figure 8**



THIS IS NOT THE FINAL VERSION - see doi:10.1042/BJ20080714